Eur. Phys. J. D **46**, 289–293 (2008)
DOI: 10.1140/epjd/e2007-00324-1

THE EUROPEAN PHYSICAL JOURNAL D

Electron impact ionization of $SiCl_2$ and SiCl

J. Mahoney[a], V. Tarnovsky, and K.H. Becker[b]

Department of Physics and Engineering Physics, Stevens Institute of Technology, Hoboken, NJ 07030, USA

Received 10 August 2007 / Received in final form 1st October 2007
Published online 5 December 2007 – © EDP Sciences, Società Italiana di Fisica, Springer-Verlag 2007

Abstract. We measured absolute partial cross sections for the formation of all singly charged positive ions produced by electron impact on $SiCl_2$ and SiCl from threshold to 200 eV using the fast-neutral-beam technique. Some of the cross section curves exhibit an unusual energy dependence with a pronounced low-energy maximum at an energy around 30 eV, which may be indicative of the presence of indirect ionization channels. Dissociative ionization channels are dominant for both species. The experimentally determined total single ionization cross sections for both species agree very well with calculated cross sections using the Deutsch-Märk (DM) formalism. A brief summary of the ionization cross sections determined for all four $SiCl_x$ ($x = 1$–4) species is given highlighting similarities and differences.

PACS. 34.80.Gs Molecular excitation and ionization by electron impact – 52.20.Fs Electron collisions

1 Introduction

The electron impact ionization and dissociative ionization of molecules and free radicals are among the important fundamental collisional interactions and they also play a key role in many applications such as gas discharges and gas lasers, fusion edge plasmas, radiation and environmental chemistry and plasma processing of materials [1–3]. We have recently reported absolute partial and total electron impact ionization cross sections for the $SiCl_4$ molecule [4] and the $SiCl_3$ free radical [5]. The work on the interactions of $SiCl_x$ ($x = 1$–4) with electrons is largely motivated by the importance of $SiCl_4$ as the main volatile etch product in chlorine-based etching of silicon [6–8]. Furthermore, $SiCl_4$ is used as an admixture in processing plasma feed gas mixtures that are used for selective reactive ion etching of GaAs on AlGaAs [9] and for other plasma-enhanced processes, including the formation of self-assembled nanocrystalline silicon dots by $SiCl_4/H_2$ plasma-enhanced chemical vapor deposition [10] and the characterization of polyester fabrics treated in $SiCl_4$ plasmas [11,12]. In all those applications, the electron-impact ionization and dissociative ionization cross sections of the $SiCl_4$ molecule, as well as of the $SiCl_x$ ($x = 1$–3) reactive species resulting from the collisional break-up of $SiCl_4$, are very important quantities for the understanding and modeling of the interaction of silicon-chlorine plasmas with materials.

In this paper we report the results of the experimental determination of absolute partial and total electron-impact ionization cross sections for $SiCl_2$ and SiCl for electron energies from threshold to 200 eV using the fast-neutral-beam technique. These measurements complement our earlier cross section determinations for $SiCl_4$ and $SiCl_3$ [4,5]. For both species, the total ionization cross section was derived as the sum of the partial cross sections. The total single ionization cross section shows very good agreement with calculated cross sections using the Deutsch-Märk (DM) formalism.

[a] *Present Address:* UV Solutions, Newark, NJ 07103, USA.
[b] *Present Address:* Polytechnic University, Brooklyn, NY 11201, USA; e-mail: `kbecker@poly.edu`

2 Experimental apparatus

We recently upgraded the fast-beam apparatus described in earlier papers [13–15] by replacing the electron gun and the ion detector. These modifications and their impact on the performance of the apparatus have been described in detail earlier [5,16] and only a brief summary will be given here. All other features of the apparatus and the experimental technique remain unchanged from what was described earlier [13–15].

The primary ion source is a commercially available Colutron ion source, in which a dc discharge between a heated filament and an anode through a suitably chosen feed gas, in this case $SiCl_4$, serves as the source of the positively charged primary ions ($SiCl_2^+$ and $SiCl^+$ in the present case). These primary ions are accelerated to about 3 keV, mass selected in a Wien filter, and sent through a charge-transfer cell filled with a suitably chosen charge-transfer gas for resonant or near-resonant charge transfer of a fraction of the primary ions. In the present case, Xe was the charge transfer gas of choice. We note that extensive earlier studies (see e.g. [17]) have shown that the exact

choice of the charge transfer gas is not crucial as long as the ionization energy of the charge transfer gas is within about ±2 eV of the ionization energy of the target species under study. The residual ions in the beam are removed from the neutral target gas beam by electrostatic deflection and most species in Rydberg states are quenched in a region of high electric field. We note that the effect of the presence of residual species in Rydberg states was studied extensively before in the case of atomic targets [13,14,18], but was found to be much less of an issue for most polyatomic molecules, which tend to have few stable (highly) excited states [17,18].

The fast neutral target beam is subsequently crossed at right angle by a well-characterized electron beam (5−200 eV beam energy, 0.25 eV FWHM energy spread, 0.1–3.0 mA beam current). The product ions are focused in the entrance plane of an electrostatic hemispherical energy analyzer which separates ions of different charge-to-mass ratios (i.e. parent ions from fragment ions). The ions leaving the analyzer travel a distance of 3.8 cm before hitting the 47-mm-diameter active area of a position-sensitive triple microchannel plate (MCP) detector. A high-transparency mesh, located about 1 cm in front of the MCP, serves to focus the product ion beam onto the MCP. Typical voltages applied to the mesh and MCP are −1 kV and −3 kV, respectively.

The fast-beam apparatus affords the capability to measure directly all quantities that determine the absolute cross section. However, we frequently use the well-established Kr or Ar absolute ionization cross sections to calibrate a pyroelectric crystal (for details, see [13, 14,17]). The calibrated crystal, in turn, is then used to determine the flux of the neutral target beam in absolute terms. In the present case, the reference gas was Ar, whose ionization cross section is known to better than about 5% [19]. As discussed in detail in our earlier publications [13,14,18,20,21], the typical uncertainty of absolute cross sections determined in the fast-beam apparatus is ±15–18%.

Table 1. Absolute partial and total single electron impact ionization cross sections for $SiCl_2$ as a function of electron energy from threshold to 200 eV.

	Ionization cross section (10^{-20} m^2)				
Electron energy (eV)	$SiCl_2^+$	$SiCl^+$	Si^+	Cl^+	Total (single)
12	0.04	0.15	–	–	0.19
14	0.38	0.33	–	–	0.71
16	0.62	0.43	–	–	1.05
18	0.79	0.49	–	0.75	2.03
20	1.07	0.58	0.002	1.19	2.84
22	1.34	0.68	0.57	1.41	4.00
24	1.58	0.83	1.23	1.52	5.16
26	1.75	0.92	1.55	1.72	5.94
28	1.99	1.10	2.05	1.85	7.00
30	2.16	1.19	2.48	1.91	7.74
32	2.24	1.26	2.75	2.00	8.25
34	2.34	1.39	3.04	2.05	8.82
36	2.40	1.44	3.33	2.14	9.31
38	2.46	1.53	3.59	2.26	9.84
40	2.49	1.64	3.75	2.29	10.17
42	2.49	1.67	3.85	2.31	10.32
44	2.51	1.72	4.00	2.38	10.61
46	2.52	1.81	4.04	2.41	10.77
48	2.52	1.93	4.07	2.44	10.96
50	2.52	1.99	4.17	2.47	11.15
52	2.54	2.08	4.27	2.49	11.37
54	2.55	2.18	4.30	2.52	11.55
56	2.56	2.21	4.36	2.57	11.70
58	2.57	2.27	4.42	2.64	11.90
60	2.58	2.33	4.48	2.67	12.07
62	2.59	2.40	4.58	2.69	12.26
64	2.61	2.42	4.67	2.71	12.41
66	2.62	2.47	4.73	2.73	12.55
68	2.63	2.51	4.80	2.73	12.67
70	2.62	2.53	4.79	2.77	12.71
80	2.61	2.60	4.79	2.84	12.84
90	2.56	2.64	4.61	2.92	12.73
100	2.50	2.63	4.48	2.91	12.51
110	2.45	2.53	4.41	2.90	12.28
120	2.40	2.43	4.22	2.79	11.85
130	2.35	2.36	4.06	2.71	11.49
140	2.30	2.27	3.91	2.62	11.10
160	2.21	2.11	3.61	2.41	10.34
180	2.12	1.94	3.32	2.22	9.60
200	2.00	1.76	3.02	1.99	8.77

3 Results and discussions

The molecular properties of the $SiCl_2$ and SiCl species are well known. We refer the reader to the standard references for information such as molecular structure and spectra, electronic structure and binding energies, molecular constants, bond dissociation energies, ionization potentials, heats of formation and other thermochemical data [22–29]. We limit the data presented here to cross sections for the formation of singly charged ions. Similar to what was found in the case of $SiCl_4$ [4] and $SiCl_3$ [5], the maximum values of the cross sections for the formation of doubly charged ions from $SiCl_2$ and SiCl are less than 0.1×10^{-20} m^2. All measured cross sections are summarized in Tables 1 and 2.

Figure 1 shows the measured partial cross sections for the formation of all singly charged ions produced by electron impact on $SiCl_2$ from threshold to 200 eV. The dominant process is the dissociative ionization leading to the formation of the Si^+ ion with a maximum cross section value of close to 5×10^{-20} m^2 at an impact energy around 75 eV. The other three cross sections curves ($SiCl_2^+$, $SiCl^+$, Cl^+) have maxima of about 2.5×10^{-20} m^2. We note that two partial cross sections curves ($SiCl_2^+$, Cl^+) exhibit a pronounced structure in the cross section shape around 30 eV. This is similar to the structures that were reported earlier in selected partial ionization cross section curves for $SiCl_4$ [4], $SiCl_3$ [5], $TiCl_4$ [18], and Cl_2 [30] and that were attributed to the presence of indirect ionization channels contributing to these cross sections. While it cannot be ruled out in, principle, that the observed structures in

Table 2. Absolute partial and total single electron impact ionization cross sections for SiCl as a function of electron energy from threshold to 200 eV.

	Ionization cross section (10^{-20} m^2)			
Electron energy (eV)	$SiCl^+$	Si^+	Cl^+	Total (single)
12	0.002	–	–	0.002
14	0.28	–	–	0.28
16	0.64	–	0.04	0.68
18	0.99	–	0.31	1.30
20	1.26	0.03	0.58	1.87
22	1.55	0.11	0.82	2.48
24	1.85	0.31	0.98	3.15
26	2.07	0.39	1.16	3.62
28	2.31	0.70	1.28	4.29
30	2.48	0.92	1.41	4.81
32	2.57	1.14	1.54	5.25
34	2.62	1.31	1.63	5.56
36	2.62	1.51	1.71	5.85
38	2.61	1.65	1.80	6.05
40	2.60	1.81	1.85	6.25
42	2.55	2.06	1.91	6.52
44	2.52	2.22	1.96	6.70
46	2.49	2.38	2.01	6.88
48	2.47	2.57	2.04	7.09
50	2.48	2.68	2.07	7.23
52	2.49	2.80	2.09	7.39
54	2.51	2.93	2.10	7.54
56	2.54	3.00	2.11	7.65
58	2.58	3.07	2.12	7.77
60	2.60	3.14	2.12	7.87
62	2.63	3.18	2.12	7.93
64	2.64	3.21	2.12	7.97
66	2.65	3.24	2.11	8.01
68	2.67	3.25	2.11	8.02
70	2.67	3.25	2.10	8.02
80	2.62	3.20	2.05	7.87
90	2.54	3.09	1.99	7.63
100	2.46	2.99	1.93	7.38
110	2.37	2.93	1.87	7.17
120	2.28	2.95	1.82	7.06
130	2.20	2.97	1.77	6.94
140	2.12	2.99	1.72	6.83
160	1.94	2.93	1.61	6.49
180	1.77	2.72	1.50	5.99
200	1.60	2.50	1.39	5.49

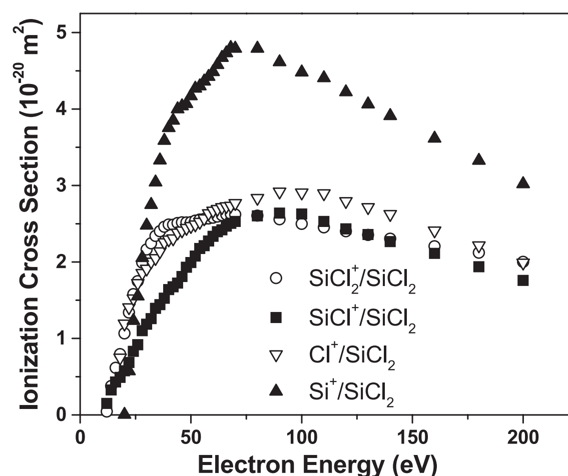

Fig. 1. Absolute partial cross sections for the formation of the singly charged ions $SiCl_2^+$ (circles), $SiCl^+$ (squares), Cl^+ (inverted triangles) and Si^+ (triangles) as a function of electron energy from threshold to 200 eV. The absolute cross sections have margins of uncertainty of ±15% (see text), which are not shown.

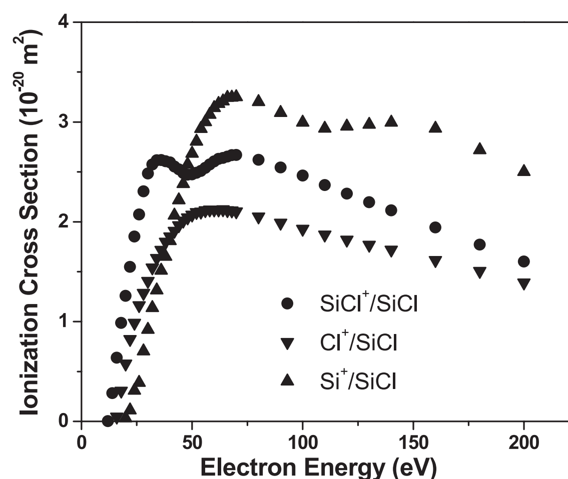

Fig. 2. Absolute partial cross sections for the formation of the singly charged ions $SiCl^+$ (circles), Cl^+ (inverted triangles) and Si^+ (triangles) as a function of electron energy from threshold to 200 eV. The absolute cross sections have margins of uncertainty of ±15% (see text), which are not shown.

the cross section curves are the result of the presence of a second direct ionization channel with a higher threshold, we do not favor this interpretation because of the energy dependence of the observed structures, which do not show the typical energy shape attributed to direct ionization processes. It is difficult to identify the exact indirect ionization channel in the present case without further studies aimed at identifying the underlying process(es). In the case of the parent $SiCl_4$ molecule [4], it was suggested [31] that the indirect ionization process proceeds via the excitation of an electron in a more tightly bound lower orbital to an unstable state above the first ionization threshold followed by the ionization of that state. The measured appearance energies for the various ions formed by electron impact on $SiCl_2$ (between 11 and 12 eV for $SiCl_2^+$ and $SiCl^+$ and slightly less than 20 eV for Cl^+ and Si^+) are all close to the thermochemical minimum energy required for the formation of the particular ion. This indicates that all ions including the Si^+ and Cl^+ atomic fragment ions are formed with little excess kinetic energy.

Figure 2 shows the measured partial cross sections from threshold to 200 eV for the formation of the $SiCl^+$, Cl^+, and Si^+ resulting from electron the impact ionization of SiCl. Here all three partial ionization cross sections have comparable maximum values, but exhibit markedly different energy dependences. The parent $SiCl^+$ and the Si^+

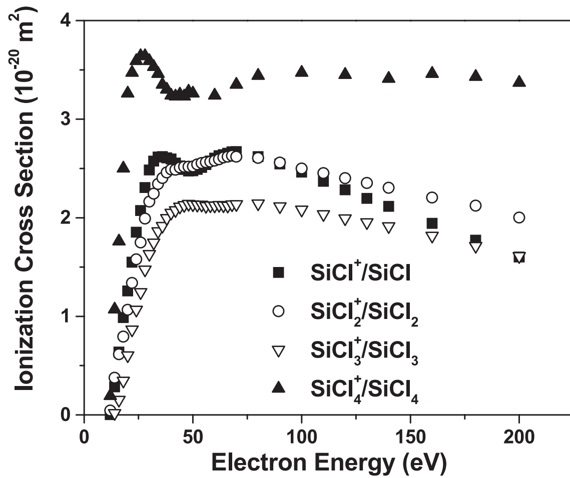

Fig. 3. Absolute partial cross sections for the formation of the singly charged parent ions $SiCl_4^+/SiCl_4$ (triangles), $SiCl_3^+/SiCl_3$ (inverted triangles), $SiCl_2^+/SiCl_2$ (circles), $SiCl^+/SiCl$ (squares) as a function of electron energy from threshold to 200 eV. The absolute cross sections have margins of uncertainty of ±15% (see text), which are not shown.

fragment cross section curves show the same pronounced structure around 30 eV mentioned above and attributed to the presence of indirect ionization channels. The measured appearance energies for the three singly charged ions formed by electron impact on SiCl (about 12 eV for $SiCl^+$ and 16 eV and 19 eV for Cl^+ and Si^+, respectively) are all close to the thermochemical minimum energy required for the formation of each ion. This indicates that all ions including the Si^+ and Cl^+ atomic fragment ions are formed with little excess kinetic energy.

We note that the presence of the indirect ionization channels that was observed in the $SiCl_2^+$ and Cl^+ partial cross sections of $SiCl_2$ and in the $SiCl^+$ and Si^+ partial cross sections of SiCl was also apparent in selected partial ionization cross section curves of $SiCl_4$ and $SiCl_3$. As an example, Figure 3 shows the four parent ionization cross sections for all $SiCl_x$ (x = 1–4) compounds. The low-energy structure is most prominent in the $SiCl_4^+$ and $SiCl^+$ parent cross sections and less pronounced for SiC_3^+ and $SiCl_2^+$.

The only comparison of the measured ionization cross sections of $SiCl_2$ and SiCl with calculated cross sections is a comparison of the total single ionization cross section (obtained as the sum of all partial cross sections for the formation of singly charged ions) with a calculated cross section using the Deutsch-Märk (DM) formalism [32]. The semi-classical DM formalism (see Deutsch et al. [33,34] and references therein to earlier publications) was originally developed for the calculation of atomic electron-impact ionization cross sections. Subsequently, Deutsch et al. [32] extended the formalism to the calculation of molecular ionization cross sections. This extension involves a molecular orbital population analysis which expresses the molecular orbitals as linear combinations of the atomic orbitals of the constituent atoms of the molecule. The result of this calculation for $SiCl_2$ and SiCl is shown

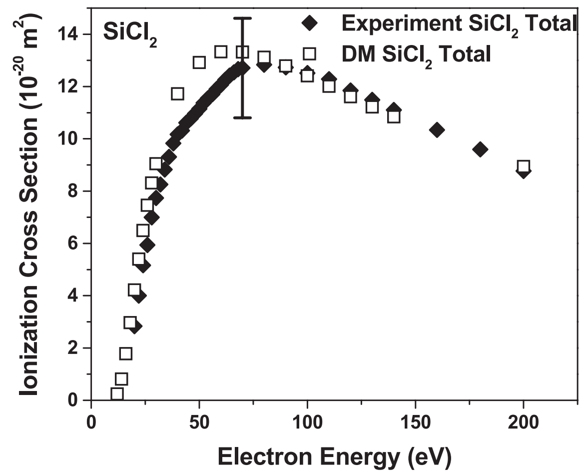

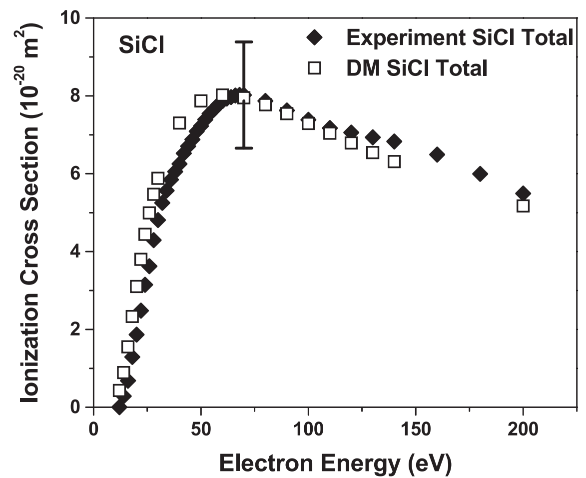

Fig. 4. Top diagram: absolute total single $SiCl_2$ ionization cross section as a function of electron energy from threshold to 200 eV, present experiment (diamonds) and calculated cross sections using the DM formalism (squares); bottom diagram: absolute total single SiCl ionization cross section as a function of electron energy from threshold to 200 eV, present experiment (diamonds) and calculated cross sections using the DM formalism (squares).

in Figure 4 (top diagram: $SiCl_2$; bottom diagram: SiCl). As can be seen, the agreement between measured and calculated total single ionization cross section is very good in both cases with regard to the absolute cross section magnitude, but somewhat less satisfactory in terms of the cross section shape. The calculated cross section rises faster as a function of electron energy and reaches its maximum value at a slightly lower electron energy. However, at any given impact energy, the deviation between calculated and measured total single ionization cross section is well within the uncertainty of the experimental cross section. Nevertheless, in view of the fact that the measured cross sections appear to include contributions from indirect ionization channels at low electron energies around 30 eV (which are not described by the DM formalism), it is surprising that the calculated DM cross sections rise faster than the experimentally determined cross sections.

Conclusions

We measured absolute partial cross sections for the formation of all singly charged ions following electron impact on $SiCl_2$ and SiCl from threshold to 200 eV using the fast-beam technique. Maximum cross section values range from 2–5 $\times 10^{-20}$ m^2. For both compounds, the partial cross section for the formation of the atomic Si^+ ion has the largest maximum cross section value. Several partial cross section curves show a prominent structure around 30 eV, which may be indicative of the presence of indirect ionization channels such as autoionization. When put into the context of our previously reported $SiCl_4$ [4] and $SiCl_3$ [5] ionization cross section studies, the following observations are noteworthy:

1. the maximum value of the total single ionization cross section increases with increasing number of Cl-atoms from 8×10^{-20} m^2 for SiCl to about 20×10^{-20} m^2 for $SiCl_4$;
2. the parent ionization cross sections for all four species are quite large (compared to those of other halogen-containing polyatomic molecules of similar molecular structure) with maximum values from 2×10^{-20} m^2 for $SiCl_3$ to almost 4×10^{-20} m^2 for $SiCl_4$, with both $SiCl_2$ and SiCl having maximum cross sections of about 2.5×10^{-20} m^2;
3. the partial cross sections for both atomic fragment ions Cl^+ and Si^+ are comparatively large for all four species, which underscores the importance of these species in plasma processing applications;
4. essentially all fragment ions resulting from the dissociative electron impact ionization of $SiCl_x$ (x = 1–4) are formed with little excess kinetic energy.

This work was supported by the Chemical Sciences, Geosciences, and Biosciences Division, Office of Basic Energy Sciences, U.S. Department of Energy.

References

1. T.D. Märk, G.H. Dunn, *Electron Impact Ionization* (Springer Verlag, Vienna, 1985)
2. L.C. Pitchford, B.V. McKoy, A. Chutjian, S. Trajmar, *Swarm Studies and Inelastic Electron-Molecule Collisions* (Srpinger Verlag, New York, 1987)
3. L.G. Christophorou, *Electron-Molecule Interactions and their Applications* (Academic Press, New York, 1984)
4. R. Basner, M. Gutkin, J. Mahoney, V. Tarnovsky, H. Deutsch, K. Becker, J. Chem. Phys. **123**, 05313 (2005)
5. J.M. Mahoney, V. Tarnovsky, K. Becker, J. Phys.: Conf. Ser., to be published
6. D. Bloor, R.J. Brook, M.C. Flemings, S. Mahajahn, R.W. Cahn, *Ion Etching and Plasma Etching of Silicon* (Pergamon, New York, 1993)
7. V.M. Donnelly, J. Appl. Phys. **79**, 9353 (1996)
8. S.J. Ullal, T.W. Kim, V. Vahedi, E.S. Aydil, J. Vac. Sci. Technol. A **21**, 589 (2003)
9. R.J. Shul, S.J. Pearton, *Handbook of Advanced Plasma Processing Techniques* (Springer, Berlin-Heidelberg, 2000)
10. Y. Fujimura, S. Jung, H. Shirai, Jpn J. Appl. Phys. **40**, 1214 (2001)
11. I.I. Negulescu, S. Despa, J. Chen, B.J. Collier, M. Despa, A. Denes, M. Sarmadi, F.S. Denes, Text. Res. J. **70**, 1 (2000)
12. L.M. Blinov, A.G. Golovkin, L.I. Kaganov, V.B. Oparin, A.A. Razhavski, A.M. Shterenberg, V.V. Volodko, V.I. Zyn, Plasma Chem. Plasma P. **18**, 509 (1998)
13. V. Tarnovsky, K. Becker, Z. Phys. D **22**, 603 (1992)
14. R.C. Wetzel, F.A. Biaocchi, T.R. Hayes, R.S. Freund, Phys. Rev. A **35**, 578 (1987)
15. T.R. Hayes, R. Shul, F.A. Biaocchi, R.S. Freund, J. Chem. Phys. **88**, 823 (1987)
16. K. Becker, J. Mahoney, M. Gutkin, V. Tarnovsky, R. Basner, Jpn J. Appl. Phys. **45**, 8818 (2006)
17. K. Becker, V. Tarnovsky, Plasma Sources Sci. Tech. **4**, 307 (1995)
18. R. Basner, M. Schmidt, V. Tarnovsky, H. Deutsch, K. Becker, Thin Solid Films **374**, 291 (2000)
19. R. Rejoub, B.G. Lindsay, R.F. Stebbings, Phys Rev. A **65**, 042713 (2002)
20. V. Tarnovsky, K. Becker, J. Chem. Phys. **98**, 7686 (1993)
21. V. Tarnovsky, P. Kurunczi, D. Rogozhnikov, K. Becker, Int. J. Mass Spectrom. **128**, 181 (1993)
22. H.M. Rosenstock, K. Draxl, B.W. Steiner, J.T. Herron, J. Phys. Chem. Ref. Data **6**, 453 (1977)
23. NIST Database (`webbook.nist.gov/chemistry/`)
24. D.R Lide, *CRC Handbook of Chemistry and Physics 2001–2002* (CRC Press, Boca Raton, FL, 2002)
25. S.G. Lias, J.E. Bartmess, J.F. Lieberman, J.L. Holmes, R.D. Levine, W.G, Mallard, J. Phys. Chem. Ref. Data **17**, 1 (1988)
26. D.D. Wagman, W.H. Evens, V.B. Parker, R.H. Schumm, I. Halow, S.M. Bailey, K.L. Chuney, R.I. Nutell, J. Phys. Chem. Ref. Data **11**, 1 (1982)
27. J.C. Speakman, *Molecules* (McGraw Hill, New York, 1966)
28. J.W. Chase, K.A. Davis, J.R. Downey, D.J. Frurip, R.A. McDonald, A.N. Syverud, J. Phys. Chem. Ref. Data **14**, 1 (1985)
29. G. Herzberg, *Molecular Structure and Molecular Spectra* (Van Reinold Nostrand, New york, 1950)
30. R. Basner, K. Becker, New J. Phys. **6**, 118 (2004)
31. T.N. Rescigno, private communication (2005)
32. H. Deutsch, K. Becker, S. Matt, T.D. Märk, Int. J. Mass Spectrom. **197**, 37 (2000), and references therein to earlier work
33. H. Deutsch, P. Scheier, K. Becker, T.D. Märk, Int. J. Mass Spectrom. **233**, 13 (2004)
34. H. Deutsch, P. Scheier, S. Matt-Leubner, K. Becker, T.D. Märk, Int. J. Mass Spectrom. **243**, 215 (2005); see also Erratum in Int. J. Mass Spectrom. **246**, 113 (2005)